



Deposited via The University of Leeds.

White Rose Research Online URL for this paper:

<https://eprints.whiterose.ac.uk/id/eprint/184638/>

Version: Accepted Version

Article:

Qian, K, Li, Z, Chakrabarty, S et al. (2023) Robust Iterative Learning Control for Pneumatic Muscle with Uncertainties and State Constraints. *IEEE Transactions on Industrial Electronics*, 70 (2). pp. 1802-1810. ISSN: 0278-0046

<https://doi.org/10.1109/TIE.2022.3159970>

© 2022 IEEE. Personal use of this material is permitted. Permission from IEEE must be obtained for all other uses, in any current or future media, including reprinting/republishing this material for advertising or promotional purposes, creating new collective works, for resale or redistribution to servers or lists, or reuse of any copyrighted component of this work in other works.

Reuse

Items deposited in White Rose Research Online are protected by copyright, with all rights reserved unless indicated otherwise. They may be downloaded and/or printed for private study, or other acts as permitted by national copyright laws. The publisher or other rights holders may allow further reproduction and re-use of the full text version. This is indicated by the licence information on the White Rose Research Online record for the item.

Takedown

If you consider content in White Rose Research Online to be in breach of UK law, please notify us by emailing eprints@whiterose.ac.uk including the URL of the record and the reason for the withdrawal request.

Robust Iterative Learning Control for Pneumatic Muscle with Uncertainties and State Constraints

Kun Qian, Zhenhong Li, Samit Chakrabarty, Zhiqiang Zhang, *Member, IEEE*,
and Sheng Quan Xie, *Senior Member, IEEE*

Abstract—In this paper, we propose a new iterative learning control (ILC) scheme for trajectory tracking of pneumatic muscle (PM) actuators with state constraints. A PM model is constructed in three-element form with both parametric and nonparametric uncertainties, while full state constraints are considered for enhancing operational safety. To ensure that system states are within the predefined bounds, the barrier Lyapunov function (BLF) is used in the analysis, which reaches infinity when some its arguments approach limits. The proposed ILC incorporates the BLF with the composite energy function (CEF) approach and ensures the boundedness of CEF in the closed-loop, thus, assuring that those limits are not transgressed. Through rigorous analysis, we show that under the proposed ILC scheme, uniform convergence of PM state tracking errors are guaranteed. Simulation studies and experimental validations are conducted to illustrate the efficacy of the proposed scheme. Experimental results show that the proposed ILC satisfies the state constraint requirements and the tracking error is less than 2.5% of the desired trajectory.

Index Terms—Iterative learning control, Pneumatic muscle, State constraint, Barrier Lyapunov function.

I. INTRODUCTION

PNEUMATIC muscles (PMs) have been actively studied in the last decades. Compared to conventional electric motors, they have advantages such as light weight, compliance and power efficiency [1]. Due to their muscle-like properties, PMs have been widely applied in robotic manipulators and rehabilitation devices [2–4]. However, its nonlinear behaviour and time-varying characteristics bring difficulties to controller design.

The three-element model [5] is commonly used to describe PM dynamics. However, the pressure-dependent uncertain parameters and unmodelled uncertainty such as friction degrade the control performance. Existing methods to handle these uncertainties include model approximation [6, 7], robust control [8, 9] and nonlinear disturbance observer (NDO) [10, 11]. To deal with parametric uncertainties, an offline model compensator is established in [6]. Alternatively, for

state-dependent nonparametric uncertainties, a state estimator is developed in [7] for feedforward controller design. Robust control schemes are proposed in [8] and [9]. Although parametric uncertainty are tackled with backstepping technique and parameter estimation algorithm, nonparametric uncertainties are not considered. To handle both uncertainties, NDOs are incorporated with dynamic surface control [10] and proxy-based sliding mode control [11]. However, the nonparametric uncertainties are assumed to be bounded by some known values which are hard to justify.

Repetitive tasks are commonly seen in industrial manufacturing and robot-aided rehabilitation [1–4]. Iterative learning control (ILC) shows superiority in handling repetitive control process [12–14]. However, the implementation of ILC on PM systems is rare. The norm-optimal ILC (NOILC) is introduced for PM tracking by minimizing an iteration-dependent quadratic function [15]. Since the computation of matrix gain requires explicit system knowledge, parametric uncertainties can not be handled. A recent study [16] establishes a data-driven model for PM and achieves position tracking by model-free adaptive iterative control (MFAILC). Although the perturbation of uncertain parameters are captured by the data-driven model, the global Lipschitz continuous (GLC) condition is required and nonparametric uncertainties are not considered. To address these problems, the composite energy function (CEF) framework [17] is introduced. CEF is originated from Lyapunov function (LF) and subsequently extended to consecutive learning cycles. The LF approach is applicable to local Lipschitz functions and guarantees the boundedness of system states within a finite interval. To evaluate the parametric learning effect along iteration horizon, the L^2 -norm of learning errors is also incorporated into CEF. Based on such construction, the convergence of CEF along iteration horizon guarantees the boundedness and pointwise convergence of the tracking error.

For an enhanced operational safety, the states of PM, i.e., contraction length and velocity are better to have some limits. Velocity constraints are considered for two PM-driven rehabilitation devices, where the duty cycle modification [18] and the saturation function [19] are used. For aforementioned two works, due to the lack of rigorous stability analysis, the performance of the closed-loop system is not theoretically guaranteed. Besides, full state constraints have been rarely considered for the control design of PMs.

In this paper, we consider the trajectory tracking problem of PMs with state constraints. A PM model is constructed under three-element form with both parametric and nonparametric

This work was supported in part by U.K. EPSRC under Grant EP/S019219/1 and Grant EP/V057782/1. (*Corresponding authors: Zhenhong Li; Sheng Quan Xie.*)

This work is in collaboration with the Institute of Rehabilitation Engineering, Binzhou Medical University, Yantai, 264033, China. K. Qian, Z. Li, Y. Zhao, Z. Zhang and S. Q. Xie are with the School of Electronic and Electrical Engineering, Faculty of Engineering, University of Leeds, Leeds LS2 9JT, U.K. (e-mail: e114kq@leeds.ac.uk; Z.H.Li@leeds.ac.uk; Z.Zhang3@leeds.ac.uk; s.q.xie@leeds.ac.uk).

S. Chakrabarty is with the School of Biomedical Sciences, Faculty of Biological Sciences, University of Leeds, Leeds LS2 9JT, U.K (e-mail: S.Chakrabarty@leeds.ac.uk).

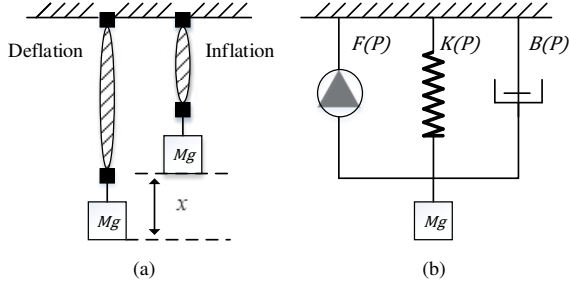


Figure 1: (a) Operational principle of a PM. (b) Three-element model of PM.

uncertainties. A new ILC scheme is proposed that consists of feedforward learning and feedback robust terms. Unlike previous results, the commonly used identical initial condition (i.i.c.) is relaxed by the alignment condition, the nonparametric uncertainties are assumed to be local Lipschitz continuous (LLC) and only lower bound of the input gain is required for the controller design. The barrier Lyapunov function (BLF) is employed to solve the constrained state tracking problem by restricting the corresponded tracking errors. With proposed sufficient conditions, we show that uniform convergence of PM state tracking errors are guaranteed, while full state constraints will not be violated through the entire learning cycle. Simulation and experimental studies are conducted to illustrate the efficacy of the proposed scheme.

The rest of paper is organized as follows. Section II formulates the state tracking problem. The proposed ILC scheme and designed CEF are developed in Section III, with rigorous convergence analysis presented by Section IV. Section V provides simulation results and experimental comparison studies.

II. PM MODELING AND PROBLEM FORMULATION

A. PM Modeling

We consider a PM that vertically drives a mass as shown in Figure 1. The system model can be described as [5]:

$$\begin{aligned} M\ddot{x}_s + B(P)\dot{x}_s + K(P)x_s &= F(P) - Mg \\ B(P) &= B_1P + B_0 = \begin{cases} B_{i1}P + B_{i0} & \text{inflation} \\ B_{d1}P + B_{d0} & \text{deflation} \end{cases} \\ K(P) &= K_1P + K_0 \\ F(P) &= F_1P + F_0 \end{aligned} \quad (1)$$

where M , P and g are the mass of load, pressure and gravitational acceleration, respectively. The PM position, velocity and acceleration are denoted as x_s , \dot{x}_s and \ddot{x}_s . $B(\cdot)$, $K(\cdot)$ and $F(\cdot)$ are the pressure-dependent damping, spring and force elements, where $B(\cdot)$ is piecewise due to inflation and deflation.

Define an equilibrium point under pressure P_0 , where the position of PM is x_0 and $\dot{x}_0 = \ddot{x}_0 = 0$, we have

$$K(P_0)x_0 = F(P_0) - Mg. \quad (2)$$

Let $u = P - P_0$ and $x = x_s - x_0$, then (1) becomes

$$\ddot{x} + \bar{B}\dot{x} + \bar{K}x = (a\dot{x} + bx + c)u \quad (3)$$

where $\bar{B} = (B_1P_0 + B_0)/M$, $\bar{K} = (K_1P_0 + K_0)/M$, $a = -B_1/M$, $b = -K_1/M$ and $c = (F_1 - K_1x_0)/M$. For PM dynamics, the pressure-dependent parameters in (1) implies that the value of \bar{B} , \bar{K} , a , b and c in (3) are unknown [8, 20]. Besides, the unmodelled uncertainty and state constraints are also crucial for a precise and safe trajectory tracking.

B. Problem Formulation

Considering the PM system works in an iterative manner with index $i \in \mathbb{N}^+$, we rewrite (3) as

$$\begin{aligned} \dot{x}_{i,1}(t) &= x_{i,2}(t) \\ \dot{x}_{i,2}(t) &= \theta^T x_i(t) + g(x_i(t))u_i + d(x_i(t), t), \quad t \in [0, T] \end{aligned} \quad (4)$$

where $T > 0$ is the time interval. $\theta = [-\bar{K}, -\bar{B}]^T$ represents the uncertain parameters and $x_i = [x_{i,1}, x_{i,2}]^T$ is a state vector. The control input is defined as u_i with unknown gain $g(x_i) = ax_{i,2} + bx_{i,1} + c$, and $d(x_i, t)$ represents the unmodelled uncertainty. The following assumptions and property are given.

Assumption 1 [21]. *The twice differentiable desired trajectory $x_{r,1}$ and its first derivative $x_{r,2}$ satisfy*

$$|x_{r,1}| \leq k_{c,1}, \quad |x_{r,2}| \leq k_{c,2}, \quad \forall t \in [0, T] \quad (5)$$

where $k_{c,1}$ and $k_{c,2}$ are two positive numbers. Note that under the desired control input u_r , the following equation similar to (4) is satisfied

$$\dot{x}_r = \theta^T x_r + g_r u_r + d_r \quad (6)$$

where $x_r = [x_{r,1}, x_{r,2}]^T$ is a desired state vector, $g_r \triangleq g(x_r)$ and $d_r \triangleq d(x_r, t)$.

Assumption 2. *Functions $g(\cdot)$ and $d(\cdot)$ in (4) satisfy LLC, that is*

$$|g(x_i) - g(x_r)| < \alpha_i \|x_i - x_r\| \quad (7)$$

$$|d(x_i) - d(x_r)| < \beta_i \|x_i - x_r\| \quad (8)$$

where $\alpha_i = \alpha(x_i, x_r, t)$ and $\beta_i = \beta(x_i, x_r, t)$ are known bounding functions and $\|\cdot\|$ is the Euclidean norm for vectors.

Assumption 3. *Reference trajectories are spatially closed, i.e., $x_{r,1}(0) = x_{r,1}(T)$, $x_{r,2}(0) = x_{r,2}(T)$. Actual trajectories are aligned, i.e., $x_{i,1}(0) = x_{i-1,1}(T)$, $x_{i,2}(0) = x_{i-1,2}(T)$.*

Property 1 [5, 8]. *For a general PM, $F_1 > 0$ always hold. Since PM's contraction range and velocity are usually small, i.e., $x_{i,1}$ and $x_{i,2}$ are small. Thus, the function $g(\cdot)$ satisfies that $g(\cdot) \geq g_{\min} > 0$.*

For safety concern, system states are required to satisfy

$$|x_{i,1}| < k_{s,1}, \quad |x_{i,2}| < k_{s,2}, \quad \forall t \in [0, T] \quad (9)$$

where $k_{s,1}$ and $k_{s,2}$ are positive state constraints. It is natural to assume that $k_{c,1} < k_{s,1}$ and $k_{c,2} < k_{s,2}$ for conducting a complete tracking. The control objective is to design a

robust constrained ILC (RCILC) controller u_i for (4) such that $x_{i,1} \rightarrow x_{r,1}$ and $x_{i,2} \rightarrow x_{r,2}$ as $i \rightarrow \infty$. All variables in the closed-loop system are global uniformly bounded and state constraints (9) are satisfied. To prevent states from violating predefined bounds, we employ BLF that incorporated with the CEF framework. The following lemma formalises a result on the use of CEF in the control design and analysis for repetitive system.

Lemma 1 [22]. For $k_{b,1}, k_{b,2} \in \mathbb{R}^+$, let $\mathcal{L} := \{(\ell_1, \ell_2) \in \mathbb{R}^2 : |\ell_1| < k_{b,1}, |\ell_2| < k_{b,2}\}$ be an open set.

Consider the dynamic system works in an iterative manner

$$\dot{z}_i = f(z_i, t), \quad i \in \mathbb{N}^+, \quad \forall t \in [0, T] \quad (10)$$

where $z_i = [z_{i,1}, z_{i,2}]^T$ and $f : \mathcal{L} \times \mathbb{R} \rightarrow \mathbb{R}^2$. Suppose that there exists a continuously differentiable function $E : \mathcal{L} \rightarrow \mathbb{R}^+$, such that

$$E(z_i) \rightarrow \infty \text{ as } |z_{i,1}| \rightarrow k_{b,1}, \quad |z_{i,2}| \rightarrow k_{b,2}. \quad (11)$$

System (10) is under the alignment condition, i.e., $z_i(0) = z_{i-1}(T)$ and $z_1(0) \in \mathcal{L}$. If the following inequalities hold:

$$\dot{E}(z_i) < \infty \text{ and } \Delta E(z_i(T)) \leq 0, \quad \forall t \in [0, T] \quad (12)$$

where $\Delta E(z_i(T)) = E(z_i(T)) - E(z_{i-1}(T))$ is the difference between two consecutive iterations, then we have

$$z_i \in \mathcal{L}, \quad \forall t \in [0, T] \text{ and } \lim_{i \rightarrow \infty} \Delta E(z_i(T)) = 0. \quad (13)$$

Proof: The boundedness of $E(z_1(0))$ and $\dot{E}(z_i) < \infty$ infer that $E(z_1(t))$ is bounded. With the alignment condition, we have $E(z_i(t))$ is bounded for all $t \in [0, T]$ and $i \in \mathbb{N}^+$. From (11), the boundedness of $E(z_i(t))$ indicates that $z_i(t)$ remains in the set \mathcal{L} , i.e., $|z_{i,1}(t)| < k_{b,1}, |z_{i,2}(t)| < k_{b,2}, \forall t \in [0, T]$.

Since $\Delta E(z_i(T)) \leq 0$, $E(z_i(T))$ is non increasing along the iteration horizon, it implies that $\lim_{i \rightarrow \infty} E(z_i(T))$ exists. With bounded $E(z_1(T))$, at k -th iteration, we have $\lim_{k \rightarrow \infty} E(z_k(T)) = E(z_1(T)) + \lim_{k \rightarrow \infty} \sum_{i=2}^k \Delta E(z_i(T)) \leq E(z_1(T))$ and $\lim_{k \rightarrow \infty} \sum_{i=2}^k \Delta E(z_i(T))$ converges. From the convergence theorem [23], as the sum of series converges, we infer that $\Delta E(z_i(T))$ converges to zero asymptotically, as $i \rightarrow \infty$. Thus, it can be seen that (13) holds. ■

Define the state tracking error $z_{i,1} = x_{i,1} - x_{r,1}$, $z_{i,2} = x_{i,2} - \sigma_i$ and $\sigma_i = x_{r,2} - \kappa_1 z_{i,1} \cos^2(\frac{\pi z_{i,1}}{2k_{b,1}})$, where $\kappa_1 > 0$ is a constant. In our subsequent design, we transfer state constraints into corresponded error constraints, that is

$$|z_{i,1}| < k_{b,1}, \quad |z_{i,2}| < k_{b,2}, \quad \forall t \in [0, T] \quad (14)$$

where $k_{b,1}$ and $k_{b,2}$ are defined as constraints on $z_{i,1}$ and $z_{i,2}$ which are chosen by

$$\begin{aligned} k_{b,1} &\leq k_{s,1} - k_{c,1} \\ k_{b,2} &\leq k_{s,2} - k_{c,2} - \kappa_1 k_{b,1}. \end{aligned} \quad (15)$$

Note that $z_{i,2}$ is a fictitious error consists of the second order state error $\dot{z}_{i,1} = x_{i,2} - x_{r,2}$ and an additional term σ_i . If $z_{i,1} \rightarrow 0$ as $i \rightarrow \infty$, we have $z_{i,2} \rightarrow \dot{z}_{i,1}$.

Remark 1. Instead of the GLC condition in PM controller designs [16, 24], the LLC condition is considered in this study. The i.i.c. is a general assumption in ILC theory [25], i.e., $z_{i,1}(0) = z_{i,2}(0) = 0$. From a practical point of view, i.i.c. can hardly be met in various circumstances. Therefore, i.i.c. is relaxed by the alignment condition in which the final state of the previous iteration becomes the initial state of the current iteration.

III. CONTROLLER DESIGN AND CEF

A. Controller Design

The state error vector is defined as $\bar{z}_i = [z_{i,1}, \dot{z}_{i,1}]^T$ and we design the following control law

$$u_i = u_i^{ilc} + u_i^r \quad (16)$$

$$\begin{aligned} u_i^r = & -\frac{1}{g_{\min}} (\alpha_i |u_i^{ilc}| \text{sgn}(z_{i,2}) \|\bar{z}_i\| + \beta_i \text{sgn}(z_{i,2}) \|\bar{z}_i\| \\ & + |\hat{\theta}_i^T| |\bar{z}_i \text{sgn}(z_{i,2}) + |\dot{x}_{r,2} - \dot{\sigma}_i| \text{sgn}(z_{i,2}) + \kappa_2 z_{i,2} \\ & + z_{i,1} \text{sgn}(z_{i,1} z_{i,2}) \cos^2(\frac{\pi z_{i,2}^2}{2k_{b,2}^2}) \cos^{-2}(\frac{\pi z_{i,1}^2}{2k_{b,1}^2})) \end{aligned} \quad (16a)$$

$$u_i^{ilc} = \text{proj}(u_{i-1}^{ilc}) - p z_{i,2} \cos^{-2}(\frac{\pi z_{i,2}^2}{2k_{b,2}^2}), \quad u_0^{ilc} = 0 \quad (16b)$$

$$\hat{\theta}_i = \text{proj}(\hat{\theta}_{i-1}) + q z_{i,2} \bar{z}_i \cos^{-2}(\frac{\pi z_{i,2}^2}{2k_{b,2}^2}), \quad \hat{\theta}_0 = 0 \quad (16c)$$

where the control law (16) consists of a robust part (16a) and two ILC parts (16b) and (16c) with positive learning gains p and q . The sgn stands for the signum function [10]. The $\kappa_2 > 0$ is a constant and the $\dot{\sigma}_i$ is given by

$$\dot{\sigma}_i = \dot{x}_{r,2} - \kappa_1 \dot{z}_{i,1} \cos^2(\frac{\pi z_{i,1}^2}{2k_{b,1}^2}) + \kappa_1 \frac{\pi z_{i,1}}{k_{b,1}^2} \sin(\frac{\pi z_{i,1}^2}{k_{b,1}^2}) \dot{z}_{i,1}. \quad (17)$$

The definition of $\text{proj}(\cdot)$ follows

$$\text{proj}(u^{ilc}) = \begin{cases} u^{ilc} & \text{if } |u^{ilc}| \leq \bar{u}^{ilc} \\ \text{sgn}(u^{ilc}) \bar{u}^{ilc} & \text{if } |u^{ilc}| > \bar{u}^{ilc} \end{cases} \quad (18)$$

and

$$\begin{aligned} \text{proj}(\hat{\theta}) &= [\text{proj}(\hat{\theta}_1), \text{proj}(\hat{\theta}_2), \dots, \text{proj}(\hat{\theta}_\ell)]^T \\ \text{proj}(\hat{\theta}_j) &= \begin{cases} \hat{\theta}_j & \text{if } |\hat{\theta}_j| \leq \bar{\theta}_j \\ \text{sgn}(\hat{\theta}_j) \bar{\theta}_j & \text{if } |\hat{\theta}_j| > \bar{\theta}_j \end{cases} \quad j = 1, 2, \dots, \ell \end{aligned} \quad (19)$$

where $\bar{u}^{ilc} \geq |u_r|_{\text{sup}}$ and $\bar{\theta}_j \geq |\theta_j|_{\text{sup}}, \forall j = 1, 2, \dots, \ell$.

Remark 2. In ILC theory, $\text{proj}(\cdot)$ is commonly used for providing uniform convergence instead of pointwise convergence [17]. In practice, the bounding information can be selected from hardware limits and large bound can lead to divergent learning transient behaviour [25, 26].

B. Composite Energy Function

In this paper, we employ following BLFs [22]:

$$V(z_{i,1}) = \frac{k_{b,1}^2}{\pi} \tan\left(\frac{\pi z_{i,1}^2}{2k_{b,1}^2}\right), |z_{i,1}(0)| < k_{b,1} \quad (20)$$

$$V(z_{i,2}) = \frac{k_{b,2}^2}{\pi} \tan\left(\frac{\pi z_{i,2}^2}{2k_{b,2}^2}\right), |z_{i,2}(0)| < k_{b,2} \quad (21)$$

which are positive definite, continuously differentiable for $|z_{i,1}| < k_{b,1}$, $|z_{i,2}| < k_{b,2}$ and will approach infinite as $|z_{i,1}| \rightarrow k_{b,1}$, $|z_{i,2}| \rightarrow k_{b,2}$. Incorporated with BLFs, CEF is designed as

$$E_i(t) = V_i^1(t) + V_i^2(t) + V_i^3(t) \quad (22)$$

$$V_i^1(t) = \frac{k_{b,1}^2}{\pi} \tan\left(\frac{\pi z_{i,1}^2}{2k_{b,1}^2}\right) + \frac{k_{b,2}^2}{\pi} \tan\left(\frac{\pi z_{i,2}^2}{2k_{b,2}^2}\right) \quad (23)$$

$$V_i^2(t) = \frac{1}{2p} \int_0^t g_r (u_i^{ilc} - u_r)^2 d\tau \quad (24)$$

$$V_i^3(t) = \frac{1}{2q} \int_0^t (\theta - \hat{\theta}_i)^T (\theta - \hat{\theta}_i) d\tau. \quad (25)$$

Remark 3. In the optimization-based ILC [27–29], the system input, output and state constraints are transformed into matrix inequality and the control law is designed by solving the constrained optimization problem. In virtue of energy-based nature, we use CEF incorporated with BLF to handle state constraints.

IV. ANALYSIS OF CONVERGENCE PROPERTY

Theorem 1. Suppose Assumption 1–3 and Property 1 hold for (4). The initial conditions satisfy $|z_{1,1}(0)| < k_{b,1}$, $|z_{1,2}(0)| < k_{b,2}$ and $k_{b,1}$, $k_{b,2}$ are selected according to (15). If the controller (16) is applied, the following results hold.

- (1) State constraints $|x_{i,1}| < k_{s,1}$ and $|x_{i,2}| < k_{s,2}$ will not be violated.
- (2) State tracking errors $z_{i,1}$ and $\dot{z}_{i,1}$ uniformly converge to zero as $i \rightarrow \infty$.
- (3) All variables in the closed-loop system are bounded.

Proof: (i) First we show that the time derivative of E_i is bounded for any iteration. From (23) we have

$$\dot{V}_i^1 = z_{i,1} \dot{z}_{i,1} \cos^{-2}\left(\frac{\pi z_{i,1}^2}{2k_{b,1}^2}\right) + z_{i,2} \dot{z}_{i,2} \cos^{-2}\left(\frac{\pi z_{i,2}^2}{2k_{b,2}^2}\right). \quad (26)$$

In light of $\dot{z}_{i,1} = z_{i,2} - \kappa_1 z_{i,1} \cos^2\left(\frac{\pi z_{i,1}^2}{2k_{b,1}^2}\right)$ and $\dot{z}_{i,2} = \ddot{z}_{i,1} + \dot{x}_{r,2} - \dot{\sigma}_i$, we obtain that

$$\begin{aligned} \dot{V}_i^1 = & z_{i,1} z_{i,2} \cos^{-2}\left(\frac{\pi z_{i,1}^2}{2k_{b,1}^2}\right) - \kappa_1 z_{i,1}^2 \\ & + \cos^{-2}\left(\frac{\pi z_{i,2}^2}{2k_{b,2}^2}\right) (z_{i,2} \ddot{z}_{i,1} + z_{i,2} (\dot{x}_{r,2} - \dot{\sigma}_i)). \end{aligned} \quad (27)$$

From (6) and Assumption 2, we have

$$\begin{aligned} z_{i,2} \ddot{z}_{i,1} &= z_{i,2} (\theta^T \bar{z}_i + (g_i u_i - g_r u_r) + (d_i - dr)) \\ z_{i,2} u_i^{ilc} (g_i - g_r) &\leq \alpha_i |z_{i,2}| |u_i^{ilc}| \|\bar{z}_i\| \\ z_{i,2} (d_i - dr) &\leq \beta_i |z_{i,2}| \|\bar{z}_i\|. \end{aligned} \quad (28)$$

Note that $g_i u_i^{ilc} - g_r u_r = u_i^{ilc} (g_i - g_r) + g_r (u_i^{ilc} - u_r)$, according to control law (16) and Property 1, we have

$$\begin{aligned} z_{i,2} \ddot{z}_{i,1} &\leq z_{i,2} \theta^T \bar{z}_i + z_{i,2} (d_i - dr) + z_{i,2} u_i^{ilc} (g_i - g_r) \\ &\quad + g_r z_{i,2} (u_i^{ilc} - u_r) - \alpha_i |z_{i,2}| |u_i^{ilc}| \|\bar{z}_i\| - \kappa_2 z_{i,2}^2 \\ &\quad - \beta_i |z_{i,2}| \|\bar{z}_i\| - |z_{i,2}| |\hat{\theta}_i^T \bar{z}_i| - |z_{i,2}| |\dot{x}_{r,2} - \dot{\sigma}_i| \\ &\quad - |z_{i,1} z_{i,2}| \cos^2\left(\frac{\pi z_{i,2}^2}{2k_{b,2}^2}\right) \cos^{-2}\left(\frac{\pi z_{i,1}^2}{2k_{b,1}^2}\right) \\ &\leq z_{i,2} \theta^T \bar{z}_i + g_r z_{i,2} (u_i^{ilc} - u_r) - \kappa_2 z_{i,2}^2 \\ &\quad - |z_{i,2}| |\hat{\theta}_i^T \bar{z}_i| - |z_{i,2}| |\dot{x}_{r,2} - \dot{\sigma}_i| \\ &\quad - |z_{i,1} z_{i,2}| \cos^2\left(\frac{\pi z_{i,2}^2}{2k_{b,2}^2}\right) \cos^{-2}\left(\frac{\pi z_{i,1}^2}{2k_{b,1}^2}\right). \end{aligned} \quad (29)$$

Substituting (29) into (27) yields

$$\begin{aligned} \dot{V}_i^1 &\leq \cos^{-2}\left(\frac{\pi z_{i,2}^2}{2k_{b,2}^2}\right) (z_{i,2} \theta^T \bar{z}_i + g_r z_{i,2} (u_i^{ilc} - u_r) \\ &\quad - |z_{i,2}| |\hat{\theta}_i^T \bar{z}_i|) - \kappa_1 z_{i,1}^2 - \kappa_2 z_{i,2}^2. \end{aligned} \quad (30)$$

From (24) and ILC law (16b), it can be derived that

$$\begin{aligned} \dot{V}_i^2(t) &= \frac{1}{2p} g_r u_r^2 + \frac{1}{2p} g_r \text{proj}(u_{i-1}^{ilc})^2 - \frac{1}{p} g_r u_r \text{proj}(u_{i-1}^{ilc}) \\ &\quad + \cos^{-2}\left(\frac{\pi z_{i,2}^2}{2k_{b,2}^2}\right) (g_r z_{i,2} u_r + \frac{1}{2} p g_r z_{i,2}^2 \cos^{-2}\left(\frac{\pi z_{i,2}^2}{2k_{b,2}^2}\right) \\ &\quad - g_r z_{i,2} \text{proj}(u_{i-1}^{ilc})) \\ &= C_1 + \cos^{-2}\left(\frac{\pi z_{i,2}^2}{2k_{b,2}^2}\right) \left(g_r z_{i,2} (u_r - \text{proj}(u_{i-1}^{ilc})) \right. \\ &\quad \left. + \frac{1}{2} p g_r z_{i,2}^2 \cos^{-2}\left(\frac{\pi z_{i,2}^2}{2k_{b,2}^2}\right) \right) \end{aligned} \quad (31)$$

where $C_1 = \frac{1}{2p} g_r u_r^2 + \frac{1}{2p} g_r \text{proj}(u_{i-1}^{ilc})^2 - \frac{1}{p} g_r u_r \text{proj}(u_{i-1}^{ilc})$.

From (25) and ILC law (16c), the derivative of V_i^3 follows

$$\begin{aligned} \dot{V}_i^3 &= \frac{1}{2q} \theta^T \theta + \frac{1}{2q} \text{proj}(\hat{\theta}_{i-1})^T \text{proj}(\hat{\theta}_{i-1}) - \frac{1}{q} \theta^T \text{proj}(\hat{\theta}_{i-1}) \\ &\quad - \cos^{-2}\left(\frac{\pi z_{i,2}^2}{2k_{b,2}^2}\right) (z_{i,2} \theta^T \bar{z}_i - z_{i,2} \text{proj}(\hat{\theta}_{i-1})^T \bar{z}_i \\ &\quad - \frac{1}{2} q z_{i,2}^2 \bar{z}_i^T \bar{z}_i \cos^{-2}\left(\frac{\pi z_{i,2}^2}{2k_{b,2}^2}\right)) \\ &= C_2 - \cos^{-2}\left(\frac{\pi z_{i,2}^2}{2k_{b,2}^2}\right) \left(z_{i,2} (\theta - \text{proj}(\hat{\theta}_{i-1}))^T \bar{z}_i \right. \\ &\quad \left. - \frac{1}{2} q z_{i,2}^2 \bar{z}_i^T \bar{z}_i \cos^{-2}\left(\frac{\pi z_{i,2}^2}{2k_{b,2}^2}\right) \right) \end{aligned} \quad (32)$$

where $C_2 = \frac{1}{2q} \text{proj}(\hat{\theta}_{i-1})^T \text{proj}(\hat{\theta}_{i-1}) - \frac{1}{q} \theta^T \text{proj}(\hat{\theta}_{i-1}) + \frac{1}{2q} \theta^T \theta$.

Substituting (30) – (32) into (22) yields

$$\begin{aligned} \dot{E}_i &= \dot{V}_i^1 + \dot{V}_i^2 + \dot{V}_i^3 \\ &\leq C_1 + C_2 + \cos^{-2}\left(\frac{\pi z_{i,2}^2}{2k_{b,2}^2}\right) (z_{i,2} (\text{proj}(\hat{\theta}_{i-1}) - \hat{\theta}_i)^T \bar{z}_i) \\ &\quad + g_r z_{i,2} (u_i^{ilc} - \text{proj}(u_{i-1}^{ilc})) \end{aligned}$$

$$\begin{aligned}
& + \frac{1}{2} \cos^{-4}\left(\frac{\pi z_{i,2}^2}{2k_{b,2}^2}\right)(pg_r z_{i,2}^2 + qz_{i,2}^2 \bar{z}_i^T \bar{z}_i) - \kappa_1 z_{i,1}^2 - \kappa_2 z_{i,2}^2 \\
= & C_1 + C_2 - \frac{1}{2} \cos^{-4}\left(\frac{\pi z_{i,2}^2}{2k_{b,2}^2}\right)(pg_r z_{i,2}^2 + qz_{i,2}^2 \bar{z}_i^T \bar{z}_i) \\
& - \kappa_1 z_{i,1}^2 - \kappa_2 z_{i,2}^2. \tag{33}
\end{aligned}$$

The $\text{proj}(\cdot)$ function ensures that C_1 and C_2 are finite which indicates that $E_i < \infty$. According to Lemma 1, we have E_i is bounded, which guarantees the state error constraints (14) hold in the i -th iteration, as BLFs incorporated will be bounded. With $k_{b,1}$ and $k_{b,2}$ selected by (15), it is straightforward to show that $|x_{i,1}| < k_{b,1} + k_{c,1} < k_{s,1}$ and $|x_{i,2}| < k_{b,2} + |\sigma_i| < k_{s,2}$. Therefore, state constraints (9) will never be violated over the entire learning cycle.

(ii) Next, we prove that CEF is non-increasing at $t = T$. The difference of $E_i(T)$ between two consecutive iterations is defined as

$$\Delta E_i(T) = \Delta V_i^1(T) + \Delta V_i^2(T) + \Delta V_i^3(T). \tag{34}$$

From (23), $\Delta V_i^1(T)$ is given by

$$\begin{aligned}
\Delta V_i^1(T) = & \frac{k_{b,1}^2}{\pi} \tan\left(\frac{\pi z_{i,1}(0)^2}{2k_{b,1}^2}\right) - \frac{k_{b,1}^2}{\pi} \tan\left(\frac{\pi z_{i-1,1}(T)^2}{2k_{b,1}^2}\right) \\
& + \int_0^T \cos^{-2}\left(\frac{\pi z_{i,1}^2}{2k_{b,1}^2}\right) z_{i,1}(\tau) \dot{z}_{i,1}(\tau) d\tau \\
& + \frac{k_{b,2}^2}{\pi} \tan\left(\frac{\pi z_{i,2}(0)^2}{2k_{b,2}^2}\right) - \frac{k_{b,2}^2}{\pi} \tan\left(\frac{\pi z_{i-1,2}(T)^2}{2k_{b,2}^2}\right) \\
& + \int_0^T \cos^{-2}\left(\frac{\pi z_{i,2}^2}{2k_{b,2}^2}\right) z_{i,2}(\tau) \dot{z}_{i,2}(\tau) d\tau. \tag{35}
\end{aligned}$$

We will omit τ in the subsequent analysis. With Assumption 3, we have

$$\Delta V_i^1(T) = \int_0^T \left(\cos^{-2}\left(\frac{\pi z_{i,1}^2}{2k_{b,1}^2}\right) z_{i,1} \dot{z}_{i,1} + \cos^{-2}\left(\frac{\pi z_{i,2}^2}{2k_{b,2}^2}\right) z_{i,2} \dot{z}_{i,2} \right) d\tau. \tag{36}$$

Employing same manners (28)–(30), we obtain that

$$\begin{aligned}
\Delta V_i^1(T) \leq & \int_0^T \left(\cos^{-2}\left(\frac{\pi z_{i,2}^2}{2k_{b,2}^2}\right) (z_{i,2} \theta^T \bar{z}_i + z_{i,2} g_r (u_i^{ilc} - u_r) \right. \\
& \left. - |\hat{\theta}_i^T \bar{z}_i| |z_{i,2}|) - \kappa_1 z_{i,1}^2 - \kappa_2 z_{i,2}^2 \right) d\tau. \tag{37}
\end{aligned}$$

For $\Delta V_i^2(T)$, note that $u_i^{ilc} + \text{proj}(u_{i-1}^{ilc}) - 2u_r \leq 2(u_i^{ilc} - u_r)$, it can be inferred that

$$\begin{aligned}
\Delta V_i^2(T) \leq & \frac{1}{2p} \int_0^T g_r (u_i^{ilc} - \text{proj}(u_{i-1}^{ilc})) (u_i^{ilc} + \text{proj}(u_{i-1}^{ilc}) \\
& - 2u_r) d\tau \\
\leq & \int_0^T \cos^{-2}\left(\frac{\pi z_{i,2}^2}{2k_{b,2}^2}\right) z_{i,2} g_r (u_r - u_i^{ilc}) d\tau. \tag{38}
\end{aligned}$$

For $\Delta V_i^3(T)$, applying the property $(a-b)^T(a-b) - (a-c)^T(a-c) = (b-c)^T(b+c-2a)$ for vector a, b and $c \in \mathbb{R}^{\ell \times 1}$,

we derive that

$$\begin{aligned}
\Delta V_i^3(T) \leq & \frac{1}{2q} \int_0^T (\hat{\theta}_i - \text{proj}(\hat{\theta}_{i-1}))^T (\hat{\theta}_i + \text{proj}(\hat{\theta}_{i-1}) \\
& - 2\theta) d\tau \\
\leq & \int_0^T \cos^{-2}\left(\frac{\pi z_{i,2}^2}{2k_{b,2}^2}\right) z_{i,2} (\hat{\theta}_i - \theta)^T \bar{z}_i d\tau. \tag{39}
\end{aligned}$$

Substituting (37)–(39) into (34) yields

$$\Delta E_i(T) \leq \int_0^T -\kappa_1 z_{i,1}^2 - \kappa_2 z_{i,2}^2 d\tau \leq 0. \tag{40}$$

According to Lemma 1, we have $\Delta E_i(T)$ asymptotically converge to zero. Therefore, from (40), we can infer that $z_{i,1}$ and $z_{i,2}$ asymptotically converge to zero in the sense of L^2 -norm, namely

$$\lim_{i \rightarrow \infty} \int_0^T z_{i,1}^2 d\tau = 0, \quad \lim_{i \rightarrow \infty} \int_0^T z_{i,2}^2 d\tau = 0, \quad t \in [0, T]. \tag{41}$$

Part.III Boundedness of involved quantities and uniform convergence of state tracking errors

Part.I shows that state constraints are solved by (14). With bounded states, the boundedness of $\dot{z}_{i,1}$ and $\dot{\sigma}_i$ are clear. Since functions $g(\cdot)$ and $d(\cdot)$ are state-dependent, their boundedness ensure that the robust term u_i^r is also bounded. With bounded u_i , $\dot{x}_{i,2}$ is bounded which implies that $\dot{z}_{i,1} = z_{i,2} + \sigma_i - \dot{x}_{r,1}$ and $\dot{z}_{i,2} = \dot{x}_{i,2} - \dot{\sigma}_i$ are finite. Since $t \in [0, T]$ is a closed set, $z_{i,1}, z_{i,2}$ are uniformly continuous, according to (41), $z_{i,1}$ and $z_{i,2}$ uniformly converge to zero, that is

$$\lim_{i \rightarrow \infty} z_{i,1}(t) = 0, \quad \lim_{i \rightarrow \infty} z_{i,2}(t) = 0, \quad t \in [0, T]. \tag{42}$$

Notice that $\sigma_i \rightarrow x_{r,2}$ as $z_{i,1} \rightarrow 0$, we have $z_{i,2} = x_{i,2} - \sigma_i \rightarrow \dot{z}_{i,1}$. Therefore, we can conclude that the second-order state error also uniformly converge to zero, that is

$$\lim_{i \rightarrow \infty} \dot{z}_{i,1}(t) = 0, \quad t \in [0, T]. \tag{43}$$

Remark 4. *The control parameters should be set to guarantee both the performance and the stability of the closed-loop system. In particular, fast convergence can be achieved by tuning p and q up, but choosing large gains are likely to cause control saturation and measurement noise in practice. Parameter κ_1 can be determined by the error constraint (15) based on practical conditions and κ_2 should be tuned accordingly for stabilizing the robust term.*

V. SIMULATION AND EXPERIMENTAL RESULTS

A. Setup and Parameter Identification

The experimental setup of the PM platform is shown in Figure 2. The PM (Festo DMSP-20-400N) vertically drive the load and is controlled by a proportional regulator (Festo VPPM-6L-V1). The displacement of the PM is measured by an encoder (Festo MLO-POT-300). The NI roboRIO is used for data acquisition and sends voltage signal to control the valve. The control program is designed on host computer using LabVIEW. Firstly, the identification of the system parameters in (1) is conducted for simulation. The identification processes

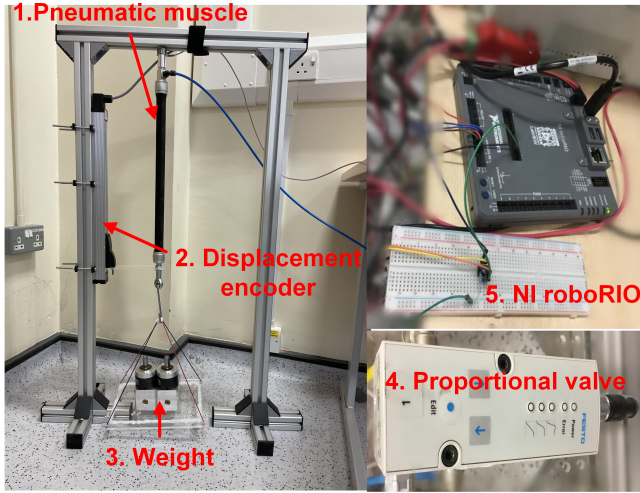


Figure 2: The PM platform contains the following components: 1. PM actuator; 2. Displacement encoder; 3. Weight (load); 4. Proportional pressure valve; 5. NI roboRIO.

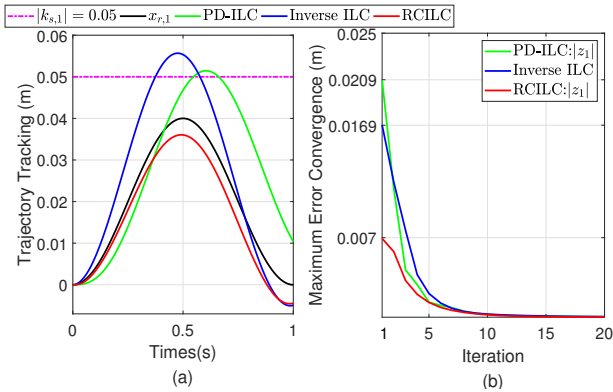


Figure 3: Simulation results. (a) Trajectory of x_1 in the first iteration; (b) Maximum error convergence within 20 iterations.

follow approaches in [20] which are omitted in this paper. The results are given by

$$\begin{aligned}
 B(P) &= \begin{cases} B_{i1}P + B_{i0} = -1.52 \times 10^{-4}P + 2829.76 \\ B_{d1}P + B_{d0} = -1.25 \times 10^{-3}P + 3068.4 \end{cases} \\
 F(P) &= F_1P + F_0 = 0.0024P - 146.8 \\
 K(P) &= \begin{cases} K_{l1}P + K_{l0} = -0.205P + 39542 \\ 0 < P \leq 1.75528 \times 10^5 Pa \\ K_{h1}P + K_{h0} = 0.025P + 1819.6 \\ 1.75528 \times 10^5 Pa < P \leq 6 \times 10^5 Pa \end{cases} \quad (44)
 \end{aligned}$$

where $K(\cdot)$ is piecewise with two sets of parameters K_{l1}, K_{l0} and K_{h1}, K_{h0} . For the simulation and experimental study, we use a 49 N load and preapply a nominal pressure $P_0 = 1.8 \times 10^5 Pa$ which will lead PM to an initial position $x_0 = 0.032 m$. For simulation, the limits of uncertain parameters in (3) can be calculated as $560.5 < \bar{B} < 1084$; $4500 < \bar{K} < 6320$; $3.74 \times 10^{-3} < a < 6.4 \times 10^{-3}$; $-3.04 \times 10^{-5} < b < -2.5 \times 10^{-4}$ and $2.75 \times 10^{-4} < c < 3.6 \times 10^{-4}$.

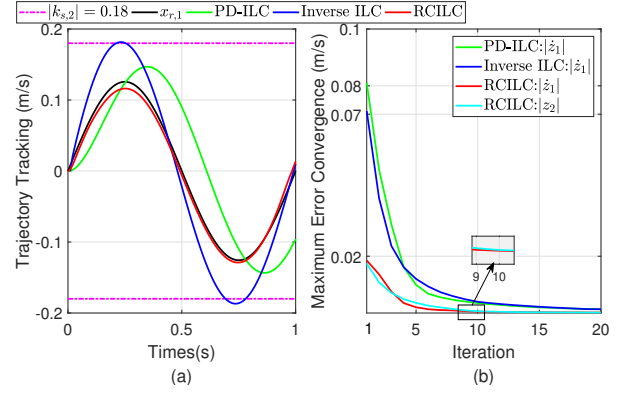


Figure 4: Simulation results. (a) Trajectory of x_2 in the first iteration; (b) Maximum error convergence within 20 iterations.

B. Simulation Study

This section validates the feasibility of the proposed control algorithm before implementing to the practical plant. The time interval in each iteration is 0.001 s and the reference trajectory is an unidirectional sine wave

$$x_{r,1} = 0.02 \sin(2\pi ft - \frac{\pi}{2}) + 0.02 \quad (45)$$

where $f = 1$ Hz and state constraints are defined as $k_{s,1} = 0.05$ and $k_{s,2} = 0.18$. Tracking results are compared with the PD-type iterative learning controller (PD-ILC) [25] and model inverse-based ILC (Inverse ILC) [30]:

$$\text{PD-ILC} : u_i = u_{i-1} + \Gamma z_{i-1,1} + \Upsilon \dot{z}_{i-1,1} \quad (46)$$

$$\text{Inverse ILC} : u_i = u_{i-1} + \Psi G^{-1} z_{i-1,1}. \quad (47)$$

where Γ , Υ and Ψ are designed learning gains and G^{-1} is the inverse of the system. Uncertainty $d(\cdot)$ in (4) is modelled as $d(x_i) = m \cdot \text{sgn}(x_{i,2}) + nx_{i,2}$, which contains Coulomb and Viscous friction with $m = 0.02$ and $n = 2$. The LLC bounding functions α_i and β_i as well as g_{min} are calculated by $\alpha_i = 0.00039$, $\beta_i = 2.02$ and $g_{min} = 5.87 \times 10^{-4}$. Control parameters of RCILC are tuned by trail and error that follows Remark 4. We first select $k_{c,1} = 0.04$ and $k_{b,1}$ is then chosen by $k_{b,1} = k_{s,1} - k_{c,1} = 0.01$. To satisfy (15), we set $k_{b,2} = 0.024$ with $\kappa_1 = 3$. The rest of the parameters are set as $p = 1 \times 10^6$, $q = 5 \times 10^4$ and $\kappa_2 = 10$. For PD-ILC and Inverse ILC, learning gains are set as $\Gamma = 6 \times 10^6$, $\Upsilon = 2 \times 10^6$ and $\Psi = 1$.

In Figure 3, tracking performances of x_1 are given. We can observe that PD-ILC and inverse ILC violate the constraint in first iteration while RCILC can restrict the state as expected. From the maximum error convergence curve, RCILC reduces the tracking error to $0.007 < k_{b,1}$ accordingly. Figure 4 shows the tracking performance of x_2 . Inverse ILC violates the constraint $k_{s,2}$ and PD-ILC has a maximum error of 0.08 m/s in first iteration, while RCILC can reduce it to 0.02 m/s according to the error constraint $k_{b,2}$. Moreover, as shown in the magnified box, RCILC uniformly converges $\dot{z}_{i,1}$ and the fictitious state error $z_{i,2}$ will approach to $\dot{z}_{i,1}$ as iteration increases.

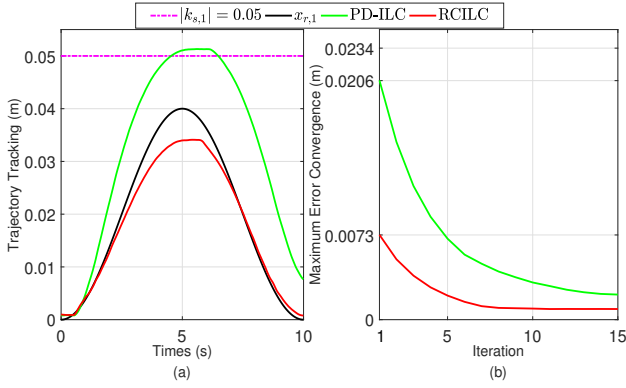


Figure 5: Experimental results. (a) Trajectory of x_1 in the first iteration; (b) Maximum error convergence within 15 iterations.

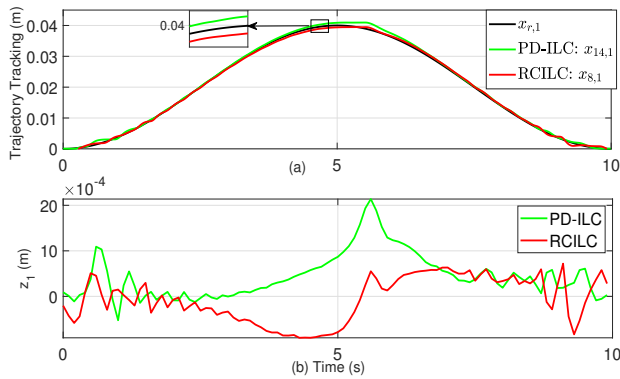


Figure 6: Tracking performance of x_1 after different iterations. (a) Trajectory of x_1 ; (b) z_1 .

C. Experimental Validation

In the experimental studies, PD-ILC and RCILC are both implemented. We first select $x_{r,1}$ with the same amplitude in (45) and set $f = 0.1$ Hz. For different frequency, experiments will also be conducted to validate the performance of the proposed scheme.

The state constraints are defined as $k_{s,1} = 0.05$, $k_{s,2} = 0.1$, while error bounds are chosen as $k_{b,1} = 0.01$, $k_{b,2} = 0.035$ with $\kappa_1 = 5$. The ILC gains in (16b) and (16c) are set as $p = 15$ and $q = 10$, and $\kappa_2 = 8$ in (16a). For the PD-ILC, the learning gains are set as $\Gamma = 75$ and $\Upsilon = 15$. In robotic applications, the position and velocity restrictions of the end-effector are essential for an enhanced safety. These restrictions can be converted into the constraints on the PM contraction range and rate, i.e., $k_{s,1}$ and $k_{s,2}$, respectively.

The trajectory tracking of x_1 in the first iteration of two schemes are shown in Figure 5(a). We can observe that the state x_1 evidently exceed the constraint 0.05 m under PD-ILC scheme. However, RCILC can avoid violation of the predefined state constraint by employing the barrier scheme. Figure 5(b) shows the maximum error convergence curves, with predefined bound $k_{b,1} = 0.01$, RCILC can quickly reduce the error accordingly implies that the employed BLF is working as expected. The tracking performance after several iterations is shown in Figure 6, we can see that both meth-

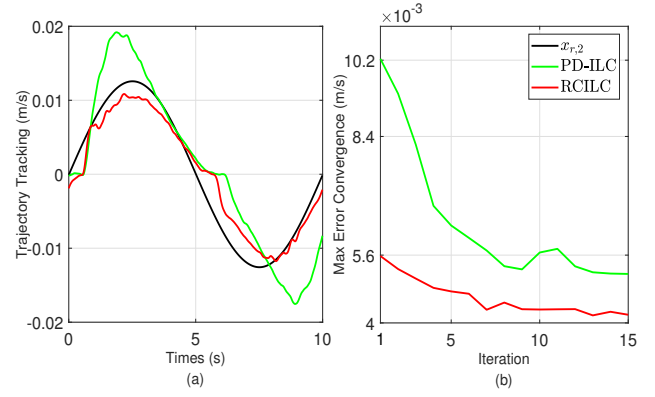


Figure 7: Experimental results. (a) Trajectory of x_2 in the first iteration; (b) Maximum error convergence within 15 iterations.

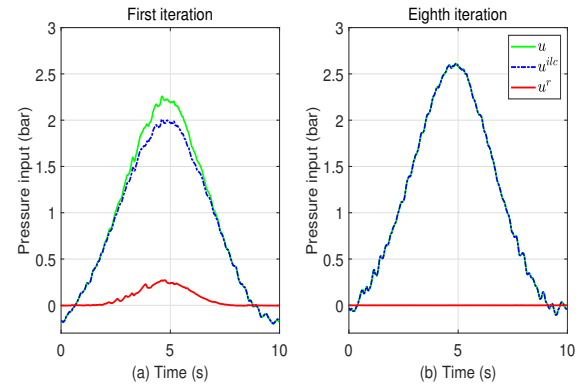


Figure 8: Control signal profiles. (a) First iteration; (b) Eighth iteration.

ods can gradually track the reference trajectory. Specifically, RCILC can reduce the tracking error to 1×10^{-3} m (2.5% of the desired trajectory) within 8 iterations, while for PD-ILC, the tracking error is 2×10^{-3} m after 14 iterations. The tracking results of $x_{i,2}$ in the first iteration and maximum error convergence curves are given in Figure 7. State x_2 is well in bound for both methods under low frequency, however, the RCILC is able to properly reduce the tracking error in the first iteration and maintain quick convergence speed.

Control input signals at the first and eighth iterations are shown in Figure 8. With large tracking error, the control effort of the robust part u^r is obvious in Figure 8(a). When the tracking error converge to a significant small level, the discrepancy between u_i and u_s^{ilc} in Figure 8(b) is also small. It indicates that, as iteration increases, the iterative learning part u_i^{ilc} will dominate the control effort.

To further verify the performance of the proposed scheme, experimental results while the PM drives different loads under different frequencies are shown in Figure 9. We can see that RCILC is able to maintain outstanding tracking performance while the state tracking error converge to approximate 1×10^{-3} m after 8 iterations for both scenarios. This indicates that the proposed scheme is practicable for various applications.

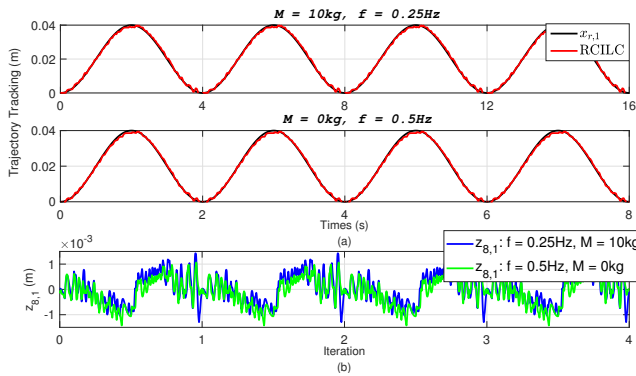


Figure 9: The tracking performance of x_1 after 8 iterations. (a) Two scenarios: 1. $M = 10\text{ kg}$, $f = 0.25\text{ Hz}$; 2. $M = 0\text{ kg}$, $f = 0.5\text{ Hz}$; (b) State tracking error z_1 under both scenarios.

VI. CONCLUSION

This paper proposes a new ILC scheme for trajectory tracking of PM actuators with predefined state constraints. Both parametric and nonparametric uncertainties are tackled and state constraints are considered for enhancing system safety. Differ from conventional ILC schemes, i.i.c. is relaxed with alignment condition and nonparametric uncertainties are assumed to be LLC. By constructing the robust feedback, the controller is designed under CEF framework and only the lower bound of the unknown control gain is required. Employing BLF approaches, we solve the state constraint problems by restricting corresponded state errors. With the given error bounds, we prove that the state tracking errors are uniformly converged and the state constraints will not be violated over the entire learning cycle. Experimental studies indicate that proposed scheme can effectively tackle state constraints and the tracking error after convergence is less than 2.5% of the desired trajectory.

REFERENCES

- [1] J. Zhang, J. Sheng, C. T. O'Neill, C. J. Walsh, R. J. Wood, J.-H. Ryu, J. P. Desai, and M. C. Yip, "Robotic artificial muscles: Current progress and future perspectives," *IEEE Trans. Robot.*, vol. 35, no. 3, pp. 761–781, 2019.
- [2] W. Meng, S. Q. Xie, Q. Liu, C. Z. Lu, and Q. Ai, "Robust iterative feedback tuning control of a compliant rehabilitation robot for repetitive ankle training," *IEEE/ASME Trans. Mechatronics*, vol. 22, no. 1, pp. 173–184, 2016.
- [3] B. Zhong, J. Cao, A. McDaid, S. Q. Xie, and M. Zhang, "Synchronous position and compliance regulation on a bi-joint gait exoskeleton driven by pneumatic muscles," *IEEE Trans. Autom. Sci. Eng.*, vol. 17, no. 4, pp. 2162–2166, 2020.
- [4] J. Kwon, S. J. Yoon, and Y.-L. Park, "Flat inflatable artificial muscles with large stroke and adjustable force-length relations," *IEEE Trans. Robot.*, vol. 36, no. 3, pp. 743–756, 2020.
- [5] D. Reynolds, D. Repperger, C. Phillips, and G. Bandry, "Modeling the dynamic characteristics of pneumatic muscle," *Ann. Biomed. Eng.*, vol. 31, no. 3, pp. 310–317, 2003.
- [6] G. Andrikopoulos, G. Nikolakopoulos, I. Arvanitakis, and S. Manesis, "Piecewise affine modeling and constrained optimal control for a pneumatic artificial muscle," *IEEE Trans. Ind. Electron.*, vol. 61, no. 2, pp. 904–916, 2013.
- [7] D. Zhang, X. Zhao, and J. Han, "Active model-based control for pneumatic artificial muscle," *IEEE Trans. Ind. Electron.*, vol. 64, no. 2, pp. 1686–1695, 2016.
- [8] L. Zhu, X. Shi, Z. Chen, H.-T. Zhang, and C.-H. Xiong, "Adaptive servomechanism of pneumatic muscle actuators with uncertainties," *IEEE Trans. Ind. Electron.*, vol. 64, no. 4, pp. 3329–3337, 2016.
- [9] N. Sun, D. Liang, Y. Wu, Y. Chen, Y. Qin, and Y. Fang, "Adaptive control for pneumatic artificial muscle systems with parametric uncertainties and unidirectional input constraints," *IEEE Trans. Ind. Informat.*, vol. 16, no. 2, pp. 969–979, 2019.
- [10] J. Wu, J. Huang, Y. Wang, and K. Xing, "Nonlinear disturbance observer-based dynamic surface control for trajectory tracking of pneumatic muscle system," *IEEE Trans. Control Syst. Technol.*, vol. 22, no. 2, pp. 440–455, 2013.
- [11] Y. Cao, C. Xiong, D. Wu, Z. Li, and Y. Hasegawa, "Adaptive proxy-based robust control integrated with nonlinear disturbance observer for pneumatic muscle actuators," *IEEE/ASME Trans. Mechatronics*, vol. 25, no. 4, pp. 1756–1764, 2020.
- [12] D. Shen and J.-X. Xu, "An iterative learning control algorithm with gain adaptation for stochastic systems," *IEEE Trans. Autom. Control*, vol. 65, no. 3, pp. 1280–1287, 2019.
- [13] S. A. Q. Mohammed, A. T. Nguyen, H. H. Choi, and J.-W. Jung, "Improved iterative learning control strategy for surface-mounted permanent magnet synchronous motor drives," *IEEE Trans. Ind. Electron.*, vol. 67, no. 12, pp. 10 134–10 144, 2020.
- [14] A. Tayebi, "Adaptive iterative learning control for robot manipulators," *Automatica*, vol. 40, no. 7, pp. 1195–1203, 2004.
- [15] D. Schindele and H. Aschemann, "ILC for a fast linear axis driven by pneumatic muscle actuators," in *2011 IEEE Int. Conf. Mechatronics*, 2011, pp. 967–972.
- [16] Q. Ai, D. Ke, J. Zuo, W. Meng, Q. Liu, Z. Zhang, and S. Q. Xie, "High-order model-free adaptive iterative learning control of pneumatic artificial muscle with enhanced convergence," *IEEE Trans. Ind. Electron.*, vol. 67, no. 11, pp. 9548–9559, 2020.
- [17] J.-X. Xu and J. Xu, "On iterative learning from different tracking tasks in the presence of time-varying uncertainties," *IEEE Trans. Syst., Man, Cybern. B*, vol. 34, no. 1, pp. 589–597, 2004.
- [18] Y.-L. Park, B.-r. Chen, N. O. Pérez-Arancibia, D. Young, L. Stirling, R. J. Wood, E. C. Goldfield, and R. Nagpal, "Design and control of a bio-inspired soft wearable robotic device for ankle-foot rehabilitation," *Bioinspir. & Biomim.*, vol. 9, no. 1, p. 016007, 2014.
- [19] Q. Liu, A. Liu, W. Meng, Q. Ai, and S. Q. Xie, "Hierarchical compliance control of a soft ankle rehabilitation robot actuated by pneumatic muscles," *Front. Neurobotics*, vol. 11, p. 64, 2017.
- [20] J. Serres, D. Reynolds, C. Phillips, M. Gerschutz, and D. Repperger, "Characterisation of a phenomenological model for commercial pneumatic muscle actuators," *Comput. Methods Biomech. Biomed. Eng.*, vol. 12, no. 4, pp. 423–430, 2009.
- [21] K. P. Tee, S. S. Ge, and E. H. Tay, "Barrier Lyapunov functions for the control of output-constrained nonlinear systems," *Automatica*, vol. 45, no. 4, pp. 918–927, 2009.
- [22] X. Jin, "Iterative learning control for non-repetitive trajectory tracking of robot manipulators with joint position constraints and actuator faults," *Int. J. Adapt. Control*, vol. 31, no. 6, pp. 859–875, 2017.
- [23] I. S. Sokolnikoff, R. M. Redheffer, and J. Avents, "Mathematics of physics and modern engineering," *J. Electrochem. Soc.*, vol. 105, no. 9, p. 196C, 1958.
- [24] Y. Yuan, Y. Yu, and L. Guo, "Nonlinear active disturbance rejection control for the pneumatic muscle actuators with discrete-time measurements," *IEEE Trans. Ind. Electron.*, vol. 66, no. 3, pp. 2044–2053, 2018.
- [25] D. A. Bristow, M. Tharayil, and A. G. Alleyne, "A survey of iterative learning control," *IEEE Control Syst. Mag.*, vol. 26, no. 3, pp. 96–114, 2006.
- [26] R. W. Longman, "Iterative learning control and repetitive control for engineering practice," *Int. J. Control*, vol. 73, no. 10, pp. 930–954, 2000.

- [27] R. Chi, X. Liu, R. Zhang, Z. Hou, and B. Huang, "Constrained data-driven optimal iterative learning control," *J. Process Control*, vol. 55, pp. 10–29, 2017.
- [28] M.-B. Radac and R.-E. Precup, "Model-free constrained data-driven iterative reference input tuning algorithm with experimental validation," *Int. J. Gen. Syst.*, vol. 45, no. 4, pp. 455–476, 2016.
- [29] C. T. Freeman and Y. Tan, "Iterative learning control with mixed constraints for point-to-point tracking," *IEEE Trans. Control Syst. Technol.*, vol. 21, no. 3, pp. 604–616, 2012.
- [30] T. Harte, J. Hätonen, and D. Owens, "Discrete-time inverse model-based iterative learning control: stability, monotonicity and robustness," *Int. J. Control*, vol. 78, no. 8, pp. 577–586, 2005.



Zhiqiang Zhang received the Ph.D. degree in electrical engineering from the University of Chinese Academy of Sciences, Beijing, China, in 2010. He was a research associate in Imperial College London for five and half years. He is an Associate Professor in body sensor networks for healthcare and robotic control with the University of Leeds, Leeds, U.K. His primary research interests are human kinematics, musculoskeletal modeling, and machine learning. He has more than 50 papers in peer-reviewed publications.



Kun Qian received a BEng degree in Electrical and Electronic Engineering and a MS degree in Digital Communication Network both from the University of Leeds, Leeds, United Kingdom, in 2016 and 2017, respectively. He is currently pursuing the Ph.D. degree with the School of Electrical and Electronic Engineering, University of Leeds. His research interests include iterative learning control, pneumatic muscle control and advanced control strategies for rehabilitation robotics.



Zhengong Li received a BEng degree in electrical engineering from Huazhong University of Science and Technology, Hubei, China, and MS and PhD degrees in control engineering from the University of Manchester, Manchester, United Kingdom, in 2014 and 2019, respectively. He is now a research fellow in the School of Electronic and Electrical Engineering at the University of Leeds. From 2018 to 2019, he was a research associate at the University of Manchester, United Kingdom. His research interests include distributed optimization, and cooperative

control of multi-agent systems.



Sheng Quan Xie received the Ph.D. degree in mechanical engineering from the University of Canterbury, Christchurch, New Zealand, in 2002. He joined the University of Auckland in 2003 and became a Chair Professor in (Bio) mechatronics in 2011. Since 2017, he has been the Chair of robotics and autonomous systems with the University of Leeds, Leeds, U.K. He has authored or coauthored eight books, 15 book chapters, and more than 400 international journal and conference papers. His current research interests include medical and rehabilitation

robots and advanced robot control. Prof. Xie is an elected Fellow of Engineering New Zealand.



Samit Chakrabarty has been studying the role of spinal circuits in execution of motor tasks, focusing on the plastic changes that the system undertakes during development or disease. After receiving his BSc in Zoology, Biochemistry from St Xavier's College, Mumbai he pursued a PhD in Neurophysiology of the mammalian spinal cord at the University of Cambridge, UK. This was then followed by postdoctoral training at Columbia University, NYC. He has since moved to University of Leeds as an academic researcher and is active in the field of sensory and

motor control and neurorehabilitation.